Prism Scanner

F. A. ROSELL
Advanced Electronics Center, General Electric Company, Ithaca, New York
(Received October 1, 1959)

The design parameters of the prism scanner appropriate to systems design are investigated analytically using a thin prism approximation and a more exact thick prism analysis. The results are specialized to the case of the spiral mode but the method is applicable to other modes.

Design equations and curves are derived for the spiral scanner using the thin prism approximation. By more exact analysis, it is shown that the thin prism analysis is adequate for preliminary design. The results are checked experimentally and are in excellent agreement.

I. INTRODUCTION

TO search a field of view with a single infrared photoconductive detector requires the use of some mechanical or optical device to provide the scan motion. The prism scanner is an example of a very versatile optical method that has the advantage of permitting a very high scan velocity and a flush mounted system. Essentially, the prism scanner consists of a pair of optical wedges, which are placed in front of the detector and optics and rotated with respect to one another. By proper adjustment of the prism velocities, at least three different scan patterns may be produced: the rosette, the spiral, and the line scan.

In this report, the spiral scan (Fig. 1) will be analyzed. The objective of the analysis is to determine analytically the parameters of the scanner for purposes of systems design and to uncover its limitations. The latter should point the way to improvement of the scanner.

In Sec. II, the prism scanner is analyzed using the thin prism approximation. The analysis results in formulas and curves for dwell time, field of view, scan redundancy, prism angular velocities, frame time, and other important design parameters.

In Sec. III, a portion of the analysis is repeated using the more exact thick prism theory, i.e., successive application of Snell's law. The thin prism approximation does not result in large errors and is satisfactory for preliminary design, as shown. The results are checked against experimental data and are in excellent agreement.

Some practical aspects of the prism scanner and suggestions are discussed in Sec. IV.

II. THIN PRISM APPROXIMATION

In an optical prism, a light-beam incident is deviated by both surfaces such that the deviation by the first surface is further increased by the second. The amount of deviation at each surface is governed by Snell's law, which states that if n_a is the index of refraction of air and n' is the index of refraction of the prism material, then

$$n_a \sin\phi_1 = n' \sin\phi', \qquad (1.01)$$
$$n_a \sin\phi_2 = n' \sin\phi_2',$$

where the geometry is as shown in Fig. 2(a). When the refracting angle of the prism is very small, it is approximately true that

$$R \cong (n'-1)\alpha^1 \quad \text{(thin prism in air)}, \qquad (1.02)$$

where R is equal to the angle ϕ_2, provided that the prism is used at or near minimum deviation. The effect of the prism on the light may be represented by a vector ρ, as shown in Fig. 3. Notice that the prism causes no lateral displacement of light along the x axis. A combination of two prisms may be used to obtain a prism of variable angle by rotating one with respect to the other. By holding one fixed and rotating the other, the resultant deviation will rotate in the xy plane as well as translate. This resultant may be determined by the vector addition of the deviations of each prism individually (Fig. 3).

Quantitatively, the resultant deviation of the light beam is given by the law of cosines,

$$\rho = (R_1^2 + R_2^2 + 2R_1R_2 \cos 2\beta)^{\frac{1}{2}}, \qquad (1.03)$$

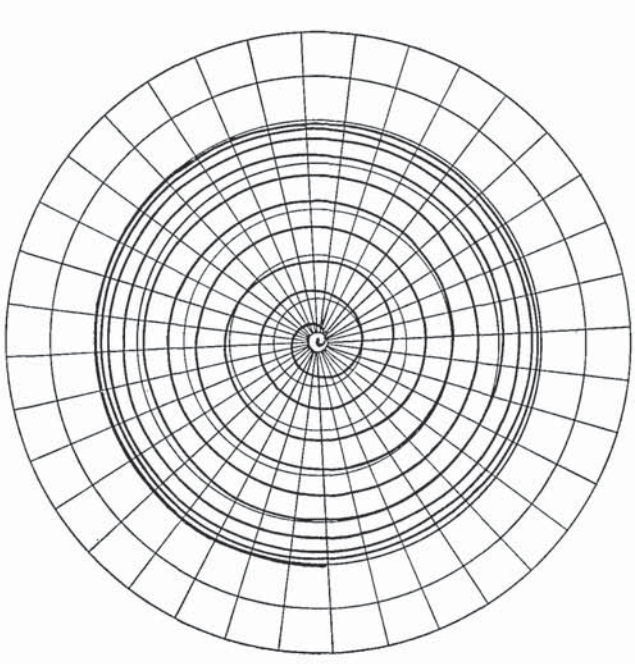

FIG. 1. Sketch of the spiral scan produced by the prism scanner with constant prism velocity and 10 revolutions per cycle.

[1] F. R. Jenkins and H. E. White, *Fundamentals of Optics* (McGraw-Hill Book Company, Inc., New York, 1950), 2nd ed., p. 31.

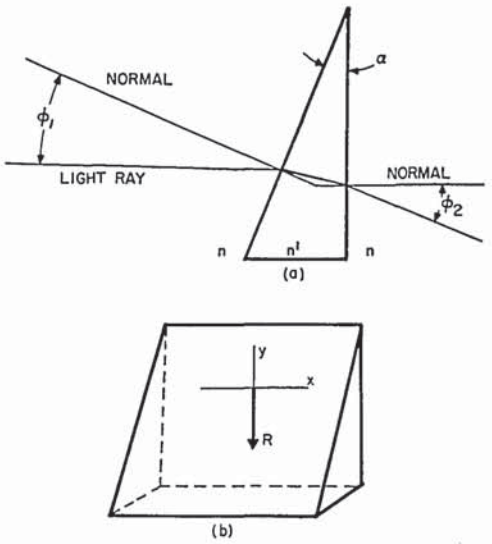

FIG. 2. Thin prism geometry and its vector equivalent.

where

$$\beta=\tfrac{1}{2}(\theta_2-\theta_1). \tag{1.04}$$

If $R_1=R_2$, then

$$\rho=2R\cos\beta. \tag{1.05}$$

Obviously, as β decreases from $\frac{1}{2}\pi$ to zero, ρ increases from 0 to $2R$ and rotates π radians in the process. A prism pair may be used in three different ways to obtain optical scanning of a field of view. In one method, the two prisms are rotated slowly relative to one another, and rapidly with respect to a common axis. This results in a spiral scan. In a second method, one is rotated rapidly and the other slowly with respect to the common axis. In this way, a rosette pattern is produced. A third method results in a line scan when both prisms are contrarotated at equal angular velocities.

A. Spiral Scan

1. Equations of Motion

In practice, it is desirable to use identical prisms and constant prism speeds. Thus

$$\begin{aligned} R_1&=R_2\\ \dot\theta_R&=\text{const}\\ \dot\theta_1&=\text{const}\\ \dot\theta_2&=\text{const}. \end{aligned} \tag{1.06}$$

By Eq. (1.03),

$$\rho=2R\cos\beta \tag{1.07}$$

$$\dot\rho=-2R\dot\beta\sin\beta. \tag{1.08}$$

From Fig. 2,

$$\dot\theta_R=\tfrac{1}{2}(\dot\theta_1+\dot\theta_2)=\dot\beta+\dot\theta_1 \tag{1.09}$$

$$\dot\beta=\tfrac{1}{2}(\dot\theta_2-\dot\theta_1). \tag{1.10}$$

For conical scan, ρ must increase from 0 to $2R$, while θ_R makes several revolutions.

2. Frame Time[2]

Frame time is defined to be equal to the time required for ρ to traverse a distance $2R$. From Eqs. (1.07) and (1.08),

$$dt=d\rho/2R\dot\beta\sin\beta$$

$$d\rho=2R\sin d\beta$$

$$\int_0^{t_f} dt=\int_0^{\frac{1}{2}\pi}\frac{d\beta}{\dot\beta}.$$

The frame time is thus

$$\begin{aligned} t_f&=\pi/2\dot\beta\\ &=\pi/(\dot\theta_2-\dot\theta_1). \end{aligned} \tag{1.11}$$

Note that

$$\dot\beta=\pi/2T_f \tag{1.12}$$

$$\beta=\pi t/2t_f \tag{1.13}$$

$$\dot\rho=(-\pi R/t_f)\sin(\pi t/2t_f). \tag{1.14}$$

3. Angular Velocities

Let θ_R make N revolutions while ρ varies from 0 to $2R$; then

$$\dot\theta_R=\tfrac{1}{2}(\dot\theta_1+\dot\theta_2)=2N\pi/t_f. \tag{1.15}$$

From Eqs. (1.10), (1.12), and (1.15),

$$\dot\theta_1=(\pi/t_f)(2N-\tfrac{1}{2}) \tag{1.16}$$

$$\dot\theta_2=(\pi/t_f)(2N+\tfrac{1}{2}). \tag{1.17}$$

4. Redundancy

Knowledge of the position of ρ on the nth revolution is desired. From Eqs. (1.13) and (1.15),

$$\theta_R=2N\pi t/t_f=2n\pi \tag{1.18}$$

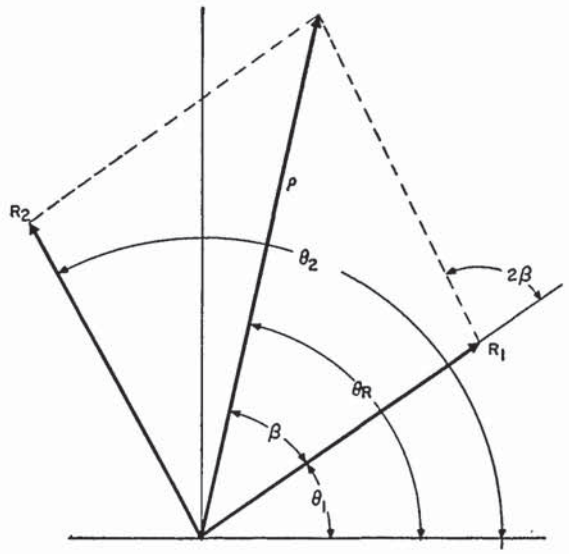

FIG. 3. Resultant deviation due to a pair of prisms from the vectorial addition of the deviation of each.

[2] This is average frame time; maximum time between successive scans at the edge of center is twice the average frame time.

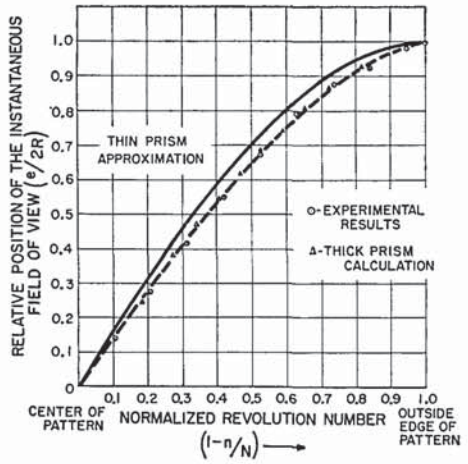

FIG. 4. Relative position of the instantaneous field of view on the Nth revolution (normalized parameters).

and

$$t=nt_f/N. \tag{1.19}$$

Substituting (1.13) and (1.19) into Eq. (1.07),

$$\begin{aligned}\rho&=2R\cos(\pi t/2t_f)\\&=2R\cos(\pi n/2N).\end{aligned} \tag{1.20}$$

Note that n is taken as zero on the outer edge of the spiral. The derivative of Eq. (1.20) is

$$d\rho/dn=(-R\pi/N)\sin(\pi n/2N), \tag{1.21}$$

which has a maximum when $n/N=1$. This value of n/N corresponds to the center of the scan. If the width of the instantaneous field of view is W deg and $\Delta n=1$ revolution, the required number of revolutions of θ_R such that there will be no spaces unseen by the detector will be

$$\begin{aligned}N&=R\pi\Delta n/\Delta\rho\\&=(R\pi/W)\text{ rev.}\end{aligned} \tag{1.22}$$

The redundancy r is

$$r=\Delta n=W/R\pi\sin[\tfrac{1}{2}\pi\cdot(n/N)]. \tag{1.23}$$

In normalized form

$$r/(W/\pi R)=1/\sin(\pi n/2N). \tag{1.24}$$

5. Scan Velocity and Dwell Time

By vector addition, the velocity of the tip vector is

$$V_\rho=[(\dot\rho)^2+(\rho\dot\theta_R)^2]^{\frac{1}{2}}. \tag{1.25}$$

Since

$$\begin{aligned}\cos\beta&=\rho/2R\\\sin\beta&=[1-(\rho/2R)^2]^{\frac{1}{2}}\\\dot\rho&=(\pi R/t_f)[1-(\rho/2R)^2]^{\frac{1}{2}}\\V_\rho&=\{(\pi R/T_f)^2[1-(\rho/2R)^2]+(2N\pi\rho/T_f)^2\}^{\frac{1}{2}}\\&=(\pi R/t_f)[1-(\rho/2R)^2+16N^2(\rho/2R)^2]^{\frac{1}{2}}\\&=(\pi R/t_f)[1+(\rho/2R)^2(16N^2-1)]^{\frac{1}{2}}.\end{aligned} \tag{1.26}$$

By definition, dwell time is the length of the instantaneous field of view (L) divided by the scan velocity:

$$\begin{aligned}td&=L/V_\rho\\&=(LT_f/\pi R)[1+(\rho/2R)^2(16N^2-1)]^{-\frac{1}{2}}.\end{aligned} \tag{1.27}$$

For $m\geq 10$ and $\rho/2R\geq 0.01$, then

$$td/(LT_f/\pi R)=1/4N(\rho/2R). \tag{1.28}$$

Note that as in the limit as ρ approaches zero, the value of Eq. (1.27 approaches $Lt_f/\pi R$.

B. Summary of Design Equations

As will be shown in the next section, the thin prism approximation is adequate for systems design purposes. Assuming the two prisms to be of equal wedge angle (α), the diameter of the field of view is $4R$ where

$$R\cong(n'-1)\alpha. \tag{1.02}$$

If both prisms are rotated at constant angular velocities $\dot\theta_1$ and $\dot\theta_2$, the frame time is

$$t_f=\pi/(\dot\theta_2-\dot\theta_1). \tag{1.11}$$

Alternately, the prism velocities are given by

$$\dot\theta_1=(\pi/t_f)(2N-\tfrac{1}{2}) \tag{1.16}$$

$$\dot\theta_2=(\pi/T_f)(2N+\tfrac{1}{2}), \tag{1.17}$$

where N is the total number of complete revolutions in the spiral from the center to the outside edge. The position of the instantaneous field of view (ρ) on the nth revolution is given by

$$\rho=2R\cos(\pi n/2N). \tag{1.18}$$

This equation is plotted in rectangular coordinates in Fig. 4, and the equivalent Eq. (1.05) is plotted in polar form in Fig. 5, except that the independent variable is taken as 2β, the angle between the prisms.

Note that in Fig. 4, experimental data form a labora-

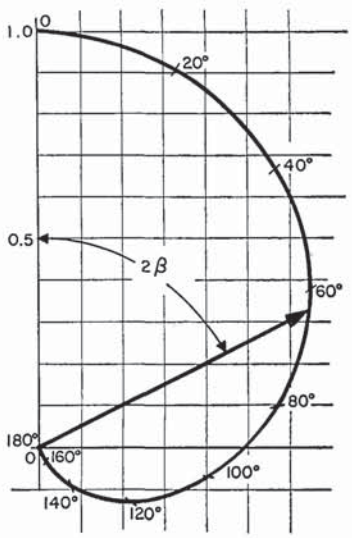

FIG. 5. Position of the instantaneous field of view vs the angle (2β) between the prism pair.

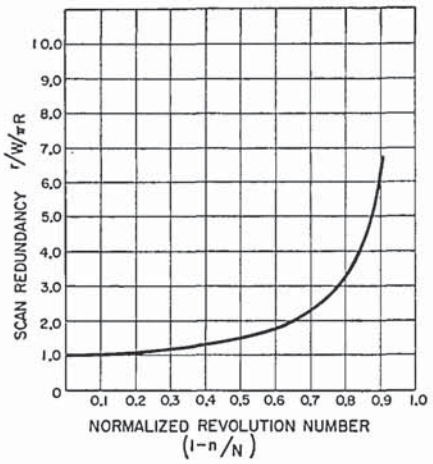

FIG. 6. Scan redundancy as a function of the rotational position of the field of view.

tory prototype is plotted. The error is discussed in Sec. III.

Scan redundancy is defined as the overlap in successive scans when the instantaneous field of view is adjusted so that no holes exist anywhere in the pattern. This redundancy (r) for an instantaneous field of view of width (W) is

$$r/(W/\pi R)=1/\sin(\pi n/2N), \tag{1.24}$$

where

$$N=R\pi/W \tag{1.22}$$

and is plotted in Fig. 6. The dwell time is given by t_d for an instantaneous field of view of length L,

$$t_d/(Lt_f/4\pi RN)=1/(\rho/2R) \tag{1.28}$$

for $\rho/2R\geq 0.01$ and $N\geq 10$. For ρ near zero,

$$\lim_{\rho/2R\to 0}\frac{td}{LT_f/4\pi RN}=4N.$$

Equation (1.28) is plotted in Fig. 7.

III. THICK PRISM ANALYSIS

The thin prism analysis holds only for small refracting angles (α) and for deviations at or near minimum. In wide field prism scanning for infrared purposes, the refracting angle is fairly large, and the index of refraction is often much larger than is normally encountered when working in the visible light spectrum. Thus, the thin prism assumption must be questioned and, if necessary, corrections made. In this analysis, a specific example will be carried along to illustrate the problems involved. For this example,

$$n'=3.00$$
$$\alpha=10°.$$

This corresponds in reality to silicon ($n'=3.42$) and to a maximum field of view of about 50 deg in radius. For purposes of analysis, consider the first prism closest to the detector to be stationary, as shown in Fig. 8.

A. Stationary Prism

The angle of the ray ϕ_2' incident on the second surface within the prism cannot exceed a critical angle. At angles less than critical, the light beam is refracted; while at larger angles of incidence, the light beam is totally reflected. By Snell's law,

$$n'\sin\phi_2'=n_\alpha\sin\phi_2. \tag{2.01}$$

At critical angle, $\phi_2=90°$, thus

$$\sin\phi_{2c}'=n_\alpha/n'. \tag{2.02}$$

For $n'=3$, $\phi_{2c}'=19.5°$, as long as the refracting angle α is smaller than ϕ_{2c}', no internal reflection will occur. Calculating angle ϕ_2, under the condition as shown in Fig. 8,

$$\begin{aligned}\sin\phi_2&=(n'/n_\alpha)\sin\phi_2'\\&=(n'/n_\alpha)\sin\alpha\\&=0.52095\end{aligned} \tag{2.03}$$

or

$$\phi_2=31.4°.$$

The deviation δ_1 is defined as

$$\begin{aligned}\delta_1&=\phi_2-\alpha\\&=21.4°.\end{aligned} \tag{2.04}$$

The main effect of prism 1 closest to the detector is to bend the light beam downward by an angle of 21.4°.

B. Rotated Prism

The second prism furthest from the detector is assumed to be of equal angle, and rotated at some arbitrary angle 2β with respect to the first, as shown in Fig. 9(a). The vector deviation δ_1 represents the bending of the light rays by prism 1. This deviation may be resolved into two components, one parallel, and one perpendicular to the thin edge of prism 2. The component $\delta_1\sin 2\beta$ in Fig. 9(b), parallel to the thin edge, is unaffected by the second prism since the prism material

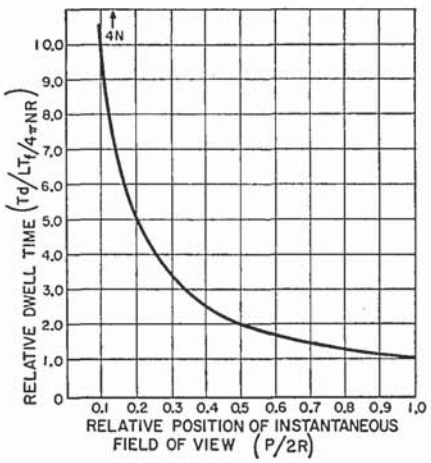

FIG. 7. Dwell time vs the position of the instantaneous field of view.

is of constant thickness with respect to this vector. The vector $\delta_1 \cos 2\beta$, perpendicular to the thin edge, is further deviated, however, as shown in Fig. 9(c).

With respect to this vector, the following relationships hold:

$$\theta_2' + \theta_1' = \alpha \tag{2.05}$$

$$\sin\theta_1 = n' \sin(\alpha - \theta_2') \tag{2.06}$$

$$\sin\theta_2 = n' \sin\theta_2' \tag{2.07}$$

$$\theta_1 = \alpha - \delta_1 \cos 2\beta. \tag{2.08}$$

Note that the angle θ_1, for the specific problem under consideration, may vary from -11.4 to 31.4 deg from Eq. (2.08).[3] The procedure for determining the magnitude of vector ρ from the equations is as follows: First note the geometry that

$$|\rho| = [(\delta_1 \sin 2\beta)^2 + \theta_2^2]^{\frac{1}{2}}. \tag{2.09}$$

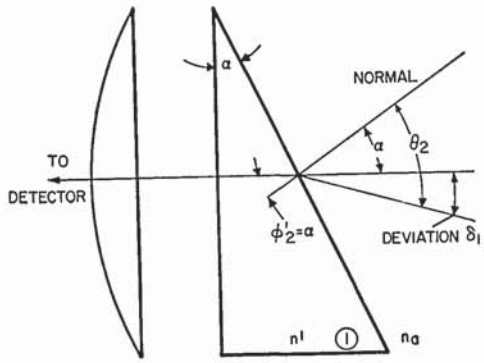

FIG. 8. For analytical purposes, prism 1 is considered stationary.

The vector δ_1 is a constant and θ_2 may be calculated as a function of β by the use of Eq. (2.05) through (2.08), since both θ_1 and α are known.

C. Results

For the case under discussion, the deviation angle θ_2 is calculated using both thick prism and thin prism analysis and the results plotted in Fig. 10 as a function of the half-angle (β) between the prisms. The conclusion obtained from this figure for the case at hand is that at most a 5% error is expected between thick angle and thin angle analysis using the normalized form of vector ρ_y, and, therefore, the thin prism approximation is valid. One result not shown because of the normalization is that the maximum total deviation, which results when the two prisms are aligned, is 45.6 deg using thick prism analysis and only 42.8 deg as predicted by the thin prism approximation.

Equation (2.09) has been calculated using the thick prism approximation, and is plotted on the curve of Fig. 4 for comparison with the experimental results and the thin prism approximation. The spread in calculated values for the thick prism is due to slide rule error. However, the agreement between the experimental results and the thick prism analysis is excellent. Note that the results are not directly comparable, because the experimental model had arsenic trisulphide prisms of 12-deg wedge angle and a 2.4 index of refraction, as opposed to the 10-deg wedge angle and an index of 3 used in calculation. In any event the method of analysis is regarded to be adequate for most purposes.

[3] A negative angle refers to an angle of incidence above the normal line.

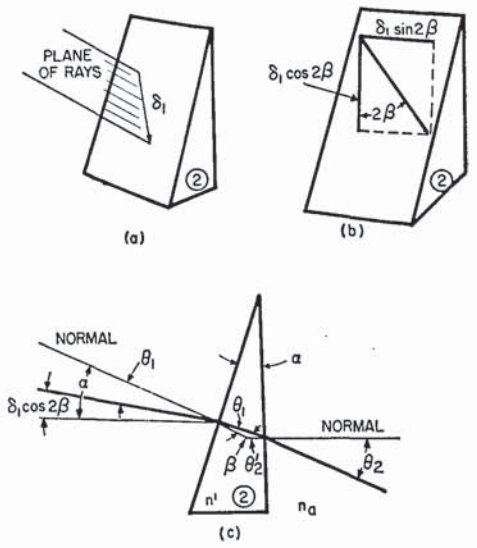

FIG. 9. Effect of prism 2 on the rays deviated by prism 1.

IV. DISCUSSION OF THE SPIRAL SCANNER

The obvious advantage of the prism scanner is that the field of view may be rapidly scanned, and flush mounting is possible. However, there are several limitations; for example, four glass surfaces are added, which reduces the optical efficiency; the dwell time is extremely nonlinear; and the scan highly redundant at the outside edge.

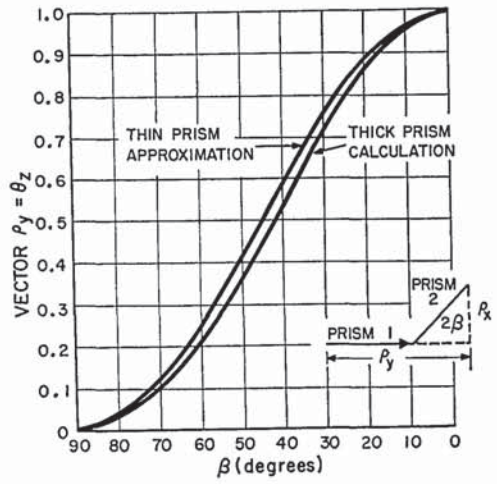

FIG. 10. Difference between thick prism analysis and the thin prism approximation for prism angles of 10 deg and index of refraction 3.

Some disadvantages not presented in this report are that the instantaneous field of view shrinks in size at the outside edge of the scanner, and that, in conversion to a track mode, conversion of the angular coordinates to a more suitable form becomes quite difficult. The prism scanner may be compensated by varying the prism velocities by the use of elliptical gearing. A certain degree of compensation may be possible in the electronics.

The extension of the analysis in this report to the rosette scan and the line scan is quite simple. The thin prism approximation is adequate for most purposes and lends itself to rapid preliminary design. With the vector notation the effect of misalignment of the prisms or unequal wedge angles can easily be determined.

V. NOMENCLATURE

Sec. II

α = prism wedge angle
β = half-angle between two prisms
$\dot{\beta}$ = rate of change of half-angle
L = length of instantaneous field of view
n = number of revolutions from outside edge of spiral scan
N = total number of revolutions outside edge to center
n_a = index of refraction of air
n' = index of refraction of prism material
R = deviation by one prism
r = scan redundancy
ρ = resultant deviation due to combination of prisms
ϕ = angle of refraction
θ = angle of prism to some stationary reference
$\dot{\theta}$ = angular velocity of prism
t = time
t_d = dwell time
T_f = frame time
V_ρ = scan velocity
W = width of instantaneous field of view

Sec. III

δ = deviation angle, one prism
θ = angle of refraction
ϕ = angle of refraction

JOURNAL OF THE OPTICAL SOCIETY OF AMERICA VOLUME 50, NUMBER 6 JUNE, 1960

Device for Maintaining the Flat-Field Relation in a Finite-Conjugate Lens Bench*

ROBERT L. LAMBERTS
Research Laboratories, Eastman Kodak Company
(Received November 9, 1959)

A lens bench is described which makes use of an electrical bridge and feedback control system to maintain the test object in a flat field for finite-conjugate operation.

RECENTLY, a lens bench was built to study lenses at finite conjugate distances in three different ways, by visual inspection of the image with a microscope, by photography, or by photoelectric scanning. The microscope, camera, and photoelectric scanning slit were made parfocal so that the same image plane would be studied by each method. Some results obtained with this equipment have already been described in this journal.[1]

GEOMETRY

In most instances, the object and image surfaces of a photographic objective operated at finite conjugates are considered to be planes perpendicular to the optical axis. To economize space, the lens is rotated on an axis that passes approximately through the second nodal point, while the test object and the image-analyzing device are kept on a fixed axis determined by a track in object space and by a precision optical bench in image space.

It can be seen from Fig. 1 that in order to maintain the necessary flat fields when the lens is rotated, two motions must be accomplished. First, the test object and the image-space apparatus must be rotated by the same amount as the lens rotates, and second, both the test object and the image-space apparatus must be moved away from the nodal pivot. Thus, the ratio of object to image distance for such flat fields is fixed and equal to the lateral magnification as the field is explored.

In image space, the longitudinal motion and rotation are accomplished by using a "tangent" or "flat-field" bar with rollers riding against its surface. The microscope for visual observations has only one roller because the field of view is very small and the microscope can remain parallel with the axis of the bench, but the camera and the photoelectric scanning device both have two rollers so that they will rotate with the lens.

* Communication No. 2064 from the Kodak Research Laboratories.

[1] Lamberts, Higgins, and Wolfe, J. Opt. Soc. Am. 48, 487 (1958); R. L. Lamberts, *ibid.* 490 (1958).